REPORT DOCUMENTATION PAGE

Form Approved OMB NO. 0704-0188

1. REPORT DATE (DD-MM-YYYY)	2. REPORT TYPE	3. DATES COVERED (From - To)
09-01-2009	Final Report	15-Jul-2004 - 14-Dec-2008

4. TITLE AND SUBTITLE

Advanced Nanocrystalline Ceramic Matrix Composites with Improved Toughness

5a. CONTRACT NUMBER
W911NF-04-1-0348

5b. GRANT NUMBER

5c. PROGRAM ELEMENT NUMBER
611102
611102

6. AUTHORS

Amiya Mukherjee, Katherine Thomson

5d. PROJECT NUMBER

5e. TASK NUMBER

5f. WORK UNIT NUMBER

7. PERFORMING ORGANIZATION NAMES AND ADDRESSES

University of California - Davis
Sponsored Programs
118 Everson Hall
Davis, CA 95616 -8671

8. PERFORMING ORGANIZATION REPORT NUMBER

9. SPONSORING/MONITORING AGENCY NAME(S) AND ADDRESS(ES)

U.S. Army Research Office
P.O. Box 12211
Research Triangle Park, NC 27709-2211

10. SPONSOR/MONITOR'S ACRONYM(S)
ARO

11. SPONSOR/MONITOR'S REPORT NUMBER(S)
44925-MS.1

12. DISTRIBUTION AVAILIBILITY STATEMENT

Approved for Public Release; Distribution Unlimited

13. SUPPLEMENTARY NOTES

The views, opinions and/or findings contained in this report are those of the author(s) and should not contrued as an official Department of the Army position, policy or decision, unless so designated by other documentation.

14. ABSTRACT

Alumina-based nanocomposites reinforced with niobium and/or carbon nanotubes were fabricated by advanced powder processing techniques and consolidated by spark plasma sintering. Raman spectroscopy revealed that single-walled carbon nanotubes (SWCNT) begin to break down at sintering temperatures above 1150°C. Nuclear magnetic resonance (NMR) showed that, although thermodynamically unlikely, no Al4C3 formed in the CNT-alumina nanocomposites. Thus, the nanocomposite is purely a physical mixture and no chemical bond was formed between the nanotubes and matrix. In addition, insitu 3-pt and standard 4-pt bend tests were conducted on niobium and/or carbon nanotube-reinforced alumina

15. SUBJECT TERMS

Nanocrystalline, Ceramics, Processing, Fracture Toughness, Carbon Nanotube, Reinforcement

16. SECURITY CLASSIFICATION OF:			17. LIMITATION OF ABSTRACT	15. NUMBER OF PAGES	19a. NAME OF RESPONSIBLE PERSON
a. REPORT	b. ABSTRACT	c. THIS PAGE			Amiya Mukherjee
U	U	U	SAR		19b. TELEPHONE NUMBER 530-752-1776

Report Title

Advanced Nanocrystalline Ceramic Matrix Composites with Improved Toughness

ABSTRACT

Alumina-based nanocomposites reinforced with niobium and/or carbon nanotubes were fabricated by advanced powder processing techniques and consolidated by spark plasma sintering. Raman spectroscopy revealed that single-walled carbon nanotubes (SWCNT) begin to break down at sintering temperatures above 1150°C. Nuclear magnetic resonance (NMR) showed that, although thermodynamically unlikely, no Al4C3 formed in the CNT-alumina nanocomposites. Thus, the nanocomposite is purely a physical mixture and no chemical bond was formed between the nanotubes and matrix. In addition, insitu 3-pt and standard 4-pt bend tests were conducted on niobium and/or carbon nanotube-reinforced alumina nanocomposites to assess their toughness. Although no subcritical crack growth was detected, average fracture toughness values of 6.1 and 3.3 MPa.m1/2 were measured for 10 vol%Nb and 10 vol%Nb-5 vol%SWCNT-alumina, respectively. Corresponding tests for the alumina nanocomposites containing 5 vol%SWCNT, 10 vol%SWCNT, 5 vol%double-walled-CNT and 10 vol% Nb yielded average fracture toughnesses of 2.95, 2.76, 3.33 and 3.95 MPa.m1/2, respectively.

List of papers submitted or published that acknowledge ARO support during this reporting period. List the papers, including journal references, in the following categories:

(a) Papers published in peer-reviewed journals (N/A for none)

1) "Processing and Characterization of Nanoceramic Composites with Interesting Structural and Functional Properties," Guo-Dong Zhan and Amiya Mukherjee, Reviews on Advanced Materials Science, vol. 10, no. 3, pp. 185-196, 2005.

2) "Thermoelectric Properties of Carbon Nanotube/Ceramic Nanocomposites," Guo-Dong Zhan, Joshua Kuntz, Amiya Mukherjee, Peixin Zhu, Kunihito Koumoto, Scripta Materialia, 54, pp. 77-82, 2005.

3) "Ultra Low-Temperature Superplasticiy in Nanoceramic Composites," Guo-Dong Zhan, Javier Garay, Amiya Mukherjee, Nano Letters, vol. 5, no 12, pp. 2593-2597, 2005.

4) "Effect of Sintering Temperature on Single-Wall Carbon Nanotube-Toughened Alumina-Based Nanocomposite," Dongtao Jiang, Katherine Thomson, Joshua Kuntz, Joel Ager, Amiya Mukherjee, Scripta Materialia, 56, pp. 959-962, 2007.

5) "A Preservation Study of Carbon Nanotues in Alumina-Based Nanocomposites via Raman Spectroscopy and Nuclear Magnetic Resonance," Katherine Thomson, Dongtao Jiang, Robert Ritchie, Amiya Mukherjee, Applied Physics A, A89, pp, 651-654, 2007.

6) "Response to Comment on "Effect of Sintering Temperature on Single-Wall Carbon Nanotube Toughened Alumina-Based Nanocomposites," Dongtao Jiang and Amiya Mukherjee, Scripta Materialia, 58, pp. 991-993, 2008.

7) "In Situ Boron Carbide-Titanium Diboride Composites Prepared by Mechanical Milling and Subsequent Spark Plasma Sintering," Dina Dudina, Dustin Hulbert, Dongtao Jiang, Cosan Unuvar, Sheldon Cytron, Amiya Mukherjee, Journal of Materials Science, 43, pp. 3569-3576, 2008.

8) "Experiments and Modeling of Spark Plasma Sintered, Functionally Graded Boron Carbide-Aluminum Composites," Dustin Hulbert, Dongtao Jiang, Umberto Anselmi-Tamburini, Cosan Unuvar, Amiya Mukherjee, Materials Science & Eng A, 488, pp. 333-338, 2008.

9) "Continuous Functionally Graded Boron Carbide-Aluminum Nanocomposites by Spark Plasma Sintering," Dustin Hulbert, Dongtao Jiang, Umberto Anselmi-Tamburini, Cosan Unuvar, Amiya Mukherjee, Materials Science & Engineering A, 493, pp. 251-255, 2008.

10) "In-Situ Bend Testing of Niobium-Reinforced Alumina Nanocomposites With and Without Single-Walled Carbon Nanotubes," Katherine Thomson, Dongtao Jiang, Joseph Lemberg, Kurt Koester, Robert Ritchie, Amiya Mukherjee, Materials Science & Engineering A, 493, pp. 256-260, 2008.

11) "The Absence of Plasma in "Spark Plasma Sintering," Dustin Hulbert, Andre Anders, Dina Dudina, Joakin Andersson, Dongtao Jiang, Cosan Unuvar, Umberto Anselmi-Tamburini, Enrique Lavernia, Amiya Mukherjee, Journal of Applied Physics, 104, pp. 033305-1 - 033305-7, 2008.

12) "The Synthesis and Consolidation of Hard Materials by Spark Plasma Sintering," Dustin Hulbert, Dongtao Jiang, Dina Dudina, Amiya Mukherjee, International Journal of Refractory & Hard Materials, 2008.

Number of Papers published in peer-reviewed journals: 12.00

(b) Papers published in non-peer-reviewed journals or in conference proceedings (N/A for none)

Number of Papers published in non peer-reviewed journals: 0.00

(c) Presentations

Number of Presentations: 0.00

Non Peer-Reviewed Conference Proceeding publications (other than abstracts):

Number of Non Peer-Reviewed Conference Proceeding publications (other than abstracts): 0

Peer-Reviewed Conference Proceeding publications (other than abstracts):

Number of Peer-Reviewed Conference Proceeding publications (other than abstracts): 0

(d) Manuscripts

"A Discussion on the Absence of Plasma in "Spark Plasma Sintering," Dustin Hulbert, Andre Anders, Joakim Andersson, Enrique Lavernia, Amiya Mukherjee, submitted to Scripta Materialia, June 2008.

Number of Manuscripts: 1.00

Number of Inventions:

Graduate Students

NAME	PERCENT_SUPPORTED
Katherine Thomson	1.00
FTE Equivalent:	**1.00**
Total Number:	**1**

Names of Post Doctorates

NAME	PERCENT_SUPPORTED
Dongtao Jiang	0.50
FTE Equivalent:	**0.50**
Total Number:	**1**

Names of Faculty Supported

NAME	PERCENT_SUPPORTED	National Academy Member
Amiya K. Mukherjee	0.13	No
FTE Equivalent:	**0.13**	
Total Number:	**1**	

Names of Under Graduate students supported

NAME	PERCENT SUPPORTED
FTE Equivalent:	
Total Number:	

Student Metrics

This section only applies to graduating undergraduates supported by this agreement in this reporting period

The number of undergraduates funded by this agreement who graduated during this period:	0.00
The number of undergraduates funded by this agreement who graduated during this period with a degree in science, mathematics, engineering, or technology fields:.....	0.00
The number of undergraduates funded by your agreement who graduated during this period and will continue to pursue a graduate or Ph.D. degree in science, mathematics, engineering, or technology fields:.....	0.00
Number of graduating undergraduates who achieved a 3.5 GPA to 4.0 (4.0 max scale):	0.00
Number of graduating undergraduates funded by a DoD funded Center of Excellence grant for Education, Research and Engineering:	0.00
The number of undergraduates funded by your agreement who graduated during this period and intend to work for the Department of Defense	0.00
The number of undergraduates funded by your agreement who graduated during this period and will receive scholarships or fellowships for further studies in science, mathematics, engineering or technology fields:	0.00

Names of Personnel receiving masters degrees

NAME
Total Number:

Names of personnel receiving PHDs

NAME
Katherine Thomson
Total Number: 1

Names of other research staff

NAME	PERCENT SUPPORTED
FTE Equivalent:	
Total Number:	

Sub Contractors (DD882)

Inventions (DD882)

Characterization and mechanical testing of alumina-based nanocomposites reinforced with niobium and/or carbon nanotubes fabricated by spark plasma sintering

K.E. Thomson[a], Dongtao Jiang[a], R.O. Ritchie[b], A.K. Mukherjee[a]
[a] Department of Chemical Engineering and Materials Science, University of California, 1 Shields Ave, Davis, CA 95616, USA
[b] Lawrence Berkeley National Laboratory, Berkeley, CA 94720 USA

Keywords: nanocomposite, carbon nanotubes, alumina, toughness, Raman spectroscopy

Abstract

Alumina-based nanocomposites reinforced with niobium and/or carbon nanotubes were fabricated by advanced powder processing techniques and consolidated by spark plasma sintering. Raman spectroscopy revealed that single-walled carbon nanotubes (SWCNT) begin to break down at sintering temperatures above 1150°C. Nuclear magnetic resonance (NMR) showed that, although thermodynamically unlikely, no Al_4C_3 formed in the CNT-alumina nanocomposites. Thus, the nanocomposite is purely a physical mixture and no chemical bond was formed between the nanotubes and matrix. In addition, *insitu* 3-pt and standard 4-pt bend tests were conducted on niobium and/or carbon nanotube-reinforced alumina nanocomposites to assess their toughness. Although no subcritical crack growth was detected, average fracture toughness values of 6.1 and 3.3 $MPa \cdot m^{1/2}$ were measured for 10 vol%Nb and 10 vol%Nb-5 vol%SWCNT-alumina, respectively. Corresponding tests for the alumina nanocomposites containing 5 vol%SWCNT, 10 vol%SWCNT, 5 vol%double-walled-CNT and 10 vol% Nb yielded average fracture toughnesses of 2.95, 2.76, 3.33 and 3.95 $MPa \cdot m^{1/2}$, respectively.

1. Introduction

The low density, chemical inertness, and high hardness/strength of nanocrystalline alumina make it an attractive candidate for compressive mechanical applications. Unfortunately, its low fracture toughness (~2.5 $MPa \cdot m^{1/2}$) impedes its utilization in such applications. The most successful approach to improving alumina's fracture toughness has been with the addition of second phases. The creation of ceramic matrix composites (CMC) has combined the high strength/hardness of alumina and toughening from the second phases by means of mechanisms such as: ductile phase toughening, fiber toughening, transformation toughening, and microcrack toughening. Over the past decade, many researchers have studied the strengthening and toughening effects of adding various metal and ceramic phases to alumina [1-15]. Only a handful of researchers have explored the potentially beneficial effects of adding carbon nanotubes to nanocrystalline alumina [16-25]. Unfortunately, the comparison of fracture toughness data is complicated by the fact that many different techniques have been used to assess the mechanical properties of these CMC. Specifically, many investigators employed the indentation fracture (IF) technique that has been proven to be unreliable and inaccurate in the past few years [26].

In this work, we investigated the effect of adding carbon nanotubes (single-walled (SWCNT) and double-walled (DWCNT)) and elemental niobium on the mechanical properties of nanocrystalline alumina with the intent of creating a tough alumina-based nanocomposite. First, it was proposed that incorporation of carbon nanotubes would provide extrinsic toughening to alumina via fiber toughening. Carbon nanotubes were chosen because they are ultra-strong due to their structural perfection, yet flexible. In addition, their conductivity and relatively high temperature resistance provide the ideal "nanocrystalline" fiber for reinforcement. Unfortunately, adequate dispersion of carbon nanotubes is very difficult due to their tendency to group into "bundles" or "ropes" of 10-100 nanotubes held together with Van der Waals forces in order to minimize surface area.

Second, it was proposed that niobium additions to nanocrystalline alumina would provide both intrinsic and extrinsic toughening via ductile-phase toughening mechanism. Niobium was chosen because its high melting temperature (~2480°C) would not compromise the potential use of alumina-based nanocomposites in high temperature applications. Investigation of the possible synergistic effects of combined toughening mechanisms, such as the ductile phase and fiber toughening mechanisms is an exciting possibility, as discussed below.

To fabricate these materials, spark plasma sintering (SPS) was used for consolidation because it avoids the excessive grain growth that would prevent obtaining a truly nanocrystalline material. SPS is an advanced, moderate pressure-assisted consolidation technique that can produce fully dense samples at lower temperatures and shorter times than conventional sintering techniques would allow. Although the mechanisms behind SPS are unclear, it is believed that a combination of rapid heating rate, pressure application, and electrical pulsing enhances the surface diffusion and thus promotes sintering of ceramic powders [27,28].

2. Experimental methods

2.1. 5 vol%SWCNT-Alumina

High energy ball-milling (HEBM) was performed on all as-received nanocrystalline alumina powder before further processing occurred. Total powder charges of ~10g of powder were loaded into a tungsten carbide (WC) vial with a single 14.3 mm WC ball and HEBMd for 24 hrs in a Spex 8000 Mixer/Mill. 1 wt% polyvinyl alcohol (PVA) was added to prevent severe powder agglomeration

during milling, but was baked out at 350°C for 3 hrs in air before further processing was performed. To prevent the carbon nanotubes' natural tendency to agglomerate, due to Van der Waals forces, 10mL of *Nanosperse* (made by NanoLab) was added to ~200mL of deionized (DI) water and mixed by hand until dissolved. The appropriate amount of single-walled carbon nanotubes (SWCNTs) produced via HiPcO method (Carbon Nanotechnologies, Inc., Texas, ~1-4 nm diameter, 90% purity) was added to the dispersant solution and ultrasonicated for ~15 mins. Simultaneously, the appropriate amount of HEBM alumina powder (NanoTek, 32nm) was added to ~200mL of ethanol, handstirred, and ultrasonicated for ~5 mins. The composite slurry was added to a polystyrene bottle with ~25 vol% zirconia ball media and wet-milled for 24 hrs. The solvent was then evaporated off on a stirring hot plate. The dispersant was baked off at 400°C for 3 hrs in air before SPS consolidation. The SPS conditions were 1200°C for 5-8 mins under 25kN load (88 MPa) and resulted in samples with relative densities from 97.7-98.3%.

2.2 5 vol%DWCNT-Alumina

Sodium dodecyl sulfate (SDS) and polyethylene glycol with a molecular weight of 2000 (PEG 2000) were used as dispersants for the double-walled carbon nanotubes (DWCNT) and nanocrystalline alumina, respectively. A 1 wt% SDS solution was created in 300 mL of DI water and 0.49 grams of DWCNT was added and ultrasonicated for 15 mins. The DWCNT (NanoLab, OD 4±1 nm, 1-5 μm length, >90% purity) were produced by chemical vapor deposition (CVD). Simultaneously, a 0.5 wt% PEG 2000 solution was made with 300 mL of DI water and 19.51 grams of HEBMd alumina (CR30, Baikalox Corp., grain size ~45 nm) added and ultrasonicated for 15mins. The two slurries were slowly combined while stirring by hand and ultrasonicated for an additional 5 mins. The composite slurry was added to a polystyrene bottle with ~25 vol% zirconia ball media and wet-milled for 24 hrs. The solvent was evaporated off on a stirring hot plate. The SDS and PEG 2000 were baked out of the powder by the following heat treatment: 1.5 hrs at 150°C, 1.5 hrs at 400°C, 12 hrs at 450°C in air, 4 hrs at 600°C in Ar, and finally 3 hrs at 850°C in Ar. The agglomerated powders were then crushed and sieved to 150 μm and consolidated via SPS. Dense (98.5%TD) samples were obtained by SPS at 1250°C for 3 mins under 30 kN load (105 MPa).

2.3. 10 vol%Nb-Alumina

In order to investigate the effectiveness of both high-energy ball milling (HEBM) and cryomilling, the 10 vol%Nb-alumina system was used compare the two techniques. The following powders were mixed by hand prior to HEBM and cryomilling: as-received alumina powder (α and γ phases, 45 nm, Baikowski International Corp.), the appropriate amount of 90 wt% Nb (99.85% purity, 74 µm, Goodfellow)-10wt% Al (99.5% purity, 45 µm, Johnson Matthey Electronics) alloy to yield a 10 vol%Nb/alumina composition, and 1 wt% polyvinyl alcohol (PVA). Aluminum was added to reduce the surface oxide of the niobium particles and PVA was added to prevent severe powder agglomeration. This powder mixture was HEBMed (Spex 8000 Mixer/Mill) for 24 hrs or cryomilled (Spex 6700 Freezer Mill) for 60 mins. The composite powders were heat treated (350°C for 3 hrs in vacuum or Ar) to remove the PVA without oxidizing the niobium. Fully dense samples (100 %TD) were obtained after SPS at 1300°C for 3 mins under 30 kN pressure (105 MPa).

2.4. 10 vol%Nb-5 vol%SWCNT-Alumina

The HEBM 10 vol%Nb-alumina composite powder from above was ultrasonicated for 15 mins in 500 mL of ethanol. The slurry was then added to a polypropylene bottle with 280 grams (~1/3 by volume) of zirconia ball media and wet-milled (130 rpm) for 24 hrs. The appropriate amount of SWCNTs (~90% purity, Carbon Nanotechnologies, Inc., Texas) was weighed out and added to a solution of 8 mL of Nanosperse (an organic surfactant made by NanoLab) and 150 mL of DI water. During final minutes of the previously-mentioned wet-milling, the SWCNT/Nanosperse aqueous solution was ultrasonicated for 5 mins. The wet-milled slurry was slowly added to the dispersed carbon nanotube solution while ultrasonicating and was added back into the polypropylene bottle and wet-milled for an additional 24 hrs.

The Nb/SWCNT/Alumina slurries were taken off the wet-mill, ball media separated, sieved through a 150 µm mesh, and placed into medium sized glass beaker. A magnetic stir bar was added and the slurry was dried on a stirring hotplate. Once dry, the agglomerates were broken up with a mortar and pestle and sieved through 150 µm mesh. In the case where Nanosperse was used, the

dispersant was baked off at 450°C for 4 hrs. The powders were consolidated with SPS into samples of 3-4 mm thickness at 1200°C for 5 mins under 30kN load (105 MPa).

2.5. Raman Spectroscopy

Pulsed Laser Raman Spectroscopy was conducted at Lawrence Berkeley National Laboratory. Spectra were detected with an imaging photomultiplier (1024×1024) with 5 cm^{-1} resolution. First, an investigation into the preservation of 10 vol%SWCNT-alumina consolidated at 1150°C for 3 mins was conducted using lasers of 522-488 nm wavelength with a 60 sec scan. Four scans were taken and overlaid for comparison of D- and G-bands: pure SWCNTs, graphite standard, pure alumina, and the 10 vol%SWCNT-alumina composite. Using the same equipment, a more in-depth Raman study was performed to identify the highest SPS condition that can be used without destroying the carbon nanotubes. This experiment was conducted using a 488 nm Ar^{+} laser line at a power of 35mW and collection times of 4 mins.

2.6. Nuclear magnetic resonance (NMR)

Nuclear magnetic resonance (NMR) was also used to investigate the carbon nanotube-alumina nanocomposites. Consolidated samples were crushed and sieved to yield powders fit for NMR study. ^{27}Al Magic Angle Spinning (MAS) NMR experiments were carried out on a Bruker Avance 500 widebore system, with the Larmor frequency of 130.32 MHz, an magic angle spinning (MAS) rate of 15 kHz, a digitization rate of 166.7 kHz, a pulse length of 0.5 μs (15 degree tip angle) and 1 sec of recycle delay, and transients of 1024. The system was calibrated with aluminum chloride solution and ~100 mg of powder were loaded into a 2.5-mm vial and analyzed under an 11.74T magnetic field.

A series of spectra were taken to investigate the local chemical environment of as-received and HEBM alumina powder, consolidated monolithic alumina, and CNT-alumina composites. Information about the interface between the carbon nanotubes and the alumina matrix was discovered in this investigation. All samples started with 32-nm Nanotek Alumina powder.

2.7. *Mechanical Testing*

Vickers indentation was used to calculate the hardness and to estimate the fracture toughness of the ceramic matrix composites in this study. A standard Tukon Microhardness tester was used with a diamond Vickers tip, a 2.278 kg load, and a dwell time of 12 secs. In most cases, the hardness and toughness crack lengths were measured on a Buehler optical microscope with the Analysis program for maximum crack resolution. The fracture toughness was calculated by measuring both diagonal lengths and crack lengths and these experimentally observed inputs were inserted into the Antis equation [29]. The average of the hardness and fracture toughness was taken from 10 or more indents.

Single-edge notched four-point bend tests were conducted using a standard servo-hydraulic MTS load frame with a 12.7-mm (0.5") displacement cartridge and a 889.6 N (200 lb-f) load cartridge. Two 3×4×19 mm beams were cut from each SPS specimen and polished to 1 μm finish. The single edge V-notched beam (SEVNB) samples were first notched using a 0.5-mm diamond saw blade to a depth of ~600 μm and the final notches were created by hand using a razor blade and1-μm diamond paste. An optical microscope was used to measure the notch depth (*a*) and notch radius of the beams. The final (*a/W*) ratios typically ranged from 0.2-0.3 and the notch radius achieved using a standard razor with diamond paste was 11-20 μm. The clean, notched beams were loaded and centered in the fixture. LabView was used to conduct the tests in displacement control and the breaking load was recorded. The beam fracture surfaces were analyzed in a FEI XL-30 SFEG scanning electron microscope (SEM).

In situ three-point bend testing was conducted to measure the extrinsic toughening effects of niobium and SWCNT additions to nanocrystalline alumina by means of ductile phase and fiber toughening, respectively. SPS samples were polished to 0.5 μm surface finish and cut into beams having dimensions of 3×4×19 mm. The SEVNB samples were pre-notched using a diamond saw, followed by an automated razor blade with 1um diamond paste to (*a/W*) ratio of 0.25-0.5. Sample preparation procedures were made in accordance with ASTM STP 1409. The pre-notched beams were three-point bend tested within a Hitachi S-4300SE/N scanning electron microscope (SEM) using a Gatan Microtest 2000 test assembly. Crack propagation was observed under a 0.55 μm/sec

loading rate. Under backscattering mode, images were recorded as the sample was loaded. Theoretically, an R-curve can be developed from a series of crack length changes at given loads. The breaking load was also recorded and the fracture toughness of the nanocomposites was calculated from stress intensity *K*-solutions in ASTM E399. The fracture surfaces were analyzed in a FEI XL-30 SFEG SEM.

3. Results and discussion

3.1. Raman spectroscopy

The results from the pulsed laser Raman spectroscopy are shown in Figs. 1 and 2. Comparison of the spectra in Fig. 1 for pure SWCNT with that of the nanocomposite consolidated at 1150°C reveals a major peak at ~1595 cm^{-1} and a shoulder in the 1550-1575 cm^{-1} region in both spectra. This is termed the "G-band" and is the tangential shear mode of the carbon atoms. The "peak splitting" of this band reflects the overlap of electrons within the graphene layers when one rolls these sheets into tubes. Thus, although the graphite peak is located in the same position as the SWCNT spectrum, it does not have splitting or a shoulder. Therefore, presence of splitting of the "G-band" indicates a nanotube structure. The minor peak at ~1350 cm^{-1} is caused by defects and the presence of amorphous carbon and can be used to quantify the purity of processed carbon nanotubes [30,31]. Clearly, the unique structure of carbon nanotubes was intact after SPS consolidation at 1150°C for 3 mins.

A more in-depth Raman study was performed to identify the highest SPS condition that can be used without destroying the carbon nanotubes. A series of spectra were taken with a 488-nm laser source at various laser powers ranging from 2 5mW to 100 mW, as shown in Fig. 2. The same G-band peak splitting is seen in the lowest temperature spectra representing consolidation at 1150°C, as located by the left dashed line. Careful analysis of Fig. 2 shows that the peak splitting disappears in the spectrum representing consolidation at 1350°C, indicating the loss of the nanotube structure. Thus, carbon-nanotube reinforced CMCs should be consolidated at temperatures below ~1250°C. This is consistent with Flahaut *et al*.'s findings in *in situ* grown CNT-Fe-Alumina nanocomposites fabricated via hot pressing [32].

3.2. Nuclear magnetic Resonance (NMR)

Analysis of the NMR spectra in Fig. 3 revealed that the aluminum atom coordination of the as-received powder was a mixture of four (at ~65 ppm) and six (at ~ 10 ppm). Close inspection of the 6-fold peak indicates that there was some distortion in the aluminum-oxygen octahedral structure due to the small amount of splitting at the top of this peak. HEBM seems to provide sufficient energy to correct this distortion because the HEBM spectra showed a clean 6-fold peak (Fig. 3b). Consequently, consolidation in the SPS at 1200°C results in complete phase transformation of the cubic 4-coordinated, metastable alumina gamma phase to the rhombohedral 6-coordinated, stable alpha phase as seen in Fig. 3c-d. The two satellite peaks in Fig. 3d are termed “spinning side bands“ and are a result of spinning and are not indicative of the chemical environment of aluminum atoms.

In addition, analysis of the carbon nanotube/alumina composite spectra for both 1200°C and 1550°C (not shown) indicated that the alumina remains 6-coordinated and that no aluminum carbide (Al_4C_3) was formed. Although thermodynamically improbable because the reaction is very slow, a peak between 20-100 ppm would have appeared if aluminum carbide were formed. In other words, the composite sample was purely a physical mixture and no chemical bonding occurred at the alumina grain/carbon nanotube interface. This is an important observation because formation of Al_4C_3 would mean breakdown of the nanotube because the nanotubes used in these studies were single-walled. Thus, the nanotubes remained as ultra-strong reinforcing fibers within the brittle alumina matrix.

3.3. Mechanical Testing

Indentation fracture (IF) testing revealed anisotropy in crack lengths and hence fracture toughness in the CMC fabricated by SPS. For example, indents were introduced to both the cross sectional and surface faces of the 10 vol%Nb-alumina sample intermixed by cryomilling. The average indentation fracture toughness and hardness calculated on the cross sectional surface was 3.46 $MPa \cdot m^{1/2}$ and 21.0 GPa, respectively. However, lower fracture toughness and slightly lower hardness was measured for the surface, specifically 2.62 $MPa \cdot m^{1/2}$ and 20.8 GPa, respectively. This corresponds to a 32% difference in fracture toughness between the surface and cross section

orientations. The samples containing 5 vol%DWCNT showed as much as 103% difference in fracture toughness when comparing surface and cross sectional indents.

In addition, there was anisotropy found within the cross sectional indents themselves. The cracks propagating in pressing direction tended to be shorter than those perpendicular to the pressing direction, indicating maximum toughness in the pressing direction. Since the alumina grains were equiaxed, the anisotropic mechanical properties are attributed to residual stresses and in the case of CMCs elongated niobium/carbon nanotube regions.

Table I shows all data collected from four-point bend testing. Both surface (s) and cross section (c.s.) orientations were measured by Vickers indentation. Table I reveals that the samples made from the cryomilled Nb-alumina powders had slightly higher fracture toughness (by about 0.40 $MPa \cdot m^{1/2}$) than those made from the HEBM powder. The IF toughness values indicate that the same anisotropy seen in DWCNT CMCs was also present in the cryomilled 10 vol%Nb-alumina samples. Regardless of milling technique, addition of 10 vol%Nb to nanocrystalline alumina was more effective in improving the intrinsic fracture toughness than carbon nanotubes were. The Nb-alumina system contained less porosity (100 %TD) and cleaner interfaces than the carbon nanotube system. The residual porosity (~1.5%) and the weakened alumina grain boundaries in the carbon nanotube system may explain the lack of intrinsic toughening. Analysis of the indents made on the 10 vol%Nb-alumina samples indicated that crack blunting was active and responsible for the improvement in intrinsic fracture toughness.

Despite the increase in carbon nanotube loading, the 10 vol%SWCNT samples displayed lower toughness than the 5 vol% samples. Among the 10 vol%SWCNT samples, the fracture toughness values increased from 2.45 to 2.76 $MPa \cdot m^{1/2}$ as the density increased from 96.4 to 97.4%TD. It is believed that the density of the samples outweighed the benefits of more reinforcing phase. Thus, obtaining full density in this material system is essential to obtaining maximum strength and toughness.

Table I. Fracture Toughness Values Determined from SEVNB Bend Testing and Indentation Fracture Methods (where *s* and *c.s.* correspond to surface and cross section orientations)

	Density	K_{IC}	Hardness	K_C (IF)
10vol%Nb-Al_2O_3	(%TD)	[MPa*m1/2]	[GPa]	[MPa*m1/2]
Cryomilled, 60min	100	3.94	s: 20.8	s: 2.6
			c.s.: 21.0	c.s.: 3.4
HEBM, 24hrs	100	3.52	s: 22.9	s: 3.3
5vol%DWCNT-Al_2O_3	98.5	3.3	s.: 20.4	s: 2.4
			c.s.: 19.0	c.s.: 4.9
SWCNT-Al_2O_3				
5vol%	99.2	2.95	c.s.: 11	c.s.: 5.0
10vol%	97.4	2.76	n/a	n/a

Also seen from Table I, DWCNT provided more intrinsic toughening than the equivalent loading of SWCNTs, *i.e.,* 3.3 vs. 2.95 MPa·$m^{1/2}$. The DWCNT sample also showed higher hardness, *i.e*., 19.0 vs. 11 GPa. Conversely, the IF method predicted nearly identical fracture toughness for the two systems. This may be attributed to the difference in fracture surfaces, as seen in Fig. 4. The SWCNTs appear to blanket the alumina grains in a weblike fashion. On the other hand, the DWCNTs have a more intimate morphology. Even with micrometer-scale CNT agglomerates, the DWCNT-alumina nanocomposites appeared more homogeneous and the CNTs were well mixed with the alumina matrix. The ropes of DWCNTs ran like tree roots into and out of the fracture surface.

Nanocrystalline alumina typically has a fracture toughness of 2.5-3.0 MPa·$m^{1/2}$. As seen in Table I, no improvement of fracture toughness was measured when 5-10 vol% SWCNTs were added to alumina. All of the values were within experimental error of that of pure alumina. This calls into question what the SEVNB method measures. We have concluded that the SEVNB method used in this study measured the load to initiate a crack and did not measure extrinsic toughening mechanisms such as fiber and grain bridging. These are precisely the toughening mechanisms that are thought to be operable in the CNT-alumina nanocomposite system. Such mechanisms have been shown before in our CNT-alumina system (Fig. 5).

Although toughening was not quantified via bend testing, a phase of three-point bend testing was conducted inside an SEM, in hopes of directly (qualitatively) observing extrinsic toughening mechanisms. Unlike most materials that possess flat R-curves, the resistance to crack propagation actually increases as the crack length increases in R-curve materials like silicon nitride, fiber

reinforced composites, and coarse grained alumina. In general, the resistance to crack propagation increases as the number of energy absorbing events increases in the crack wake.

Table II displays the sintering parameters, data collected from the *in situ* three-point bend testing, and also the hardness/fracture toughness values obtained by the IF method. All of the hardness and fracture toughness values given in Table II were calculated from the indents on the surface orientation (*i.e*., the indenter came down in the pressing direction). Although stable crack growth was not observed in these tests, the fracture toughness value obtained for 10 vol%Nb-alumina from the breaking load was 6.1 $MPa \cdot m^{1/2}$. This enhancement in fracture toughness is twice of that of monolithic alumina. However, the fracture toughness of 10 vol%Nb-alumina decreased to that of monolithic alumina when 5 vol%SWCNTs were added to the nanocomposite. Thus, there appears to be no beneficial synergy between ductile phase and fiber toughening in this system.

Table II – Summary of Mechanical Properties of In-Situ 3-pt Bend Study & IF Method

Composition	SPS Parameters	Density [% TD]	Grain Size	Indentation K_c [$MPa \cdot m^{1/2}$]	3pt Bend K_{Ic} [$MPa \cdot m^{1/2}$]	Hardness [GPa]
Al_2O_3	1300°C/3min	99.9	1.4 µm	2.7	3.1	20.9
10%Nb-Al_2O_3	1150°C/3min, 1300°C/2min	99.5	250 nm	3.3	6.1	22.9
10%Nb-5%SWCNT-Al_2O_3	1200°C/5min	98.4	580 nm	2.7	3.3	19.3

The 10 vol%Nb-5 vol%SWCNT-Al_2O_3 nanocomposites possessed a slightly larger grain size than the Nb-Al_2O_3 system due to the increase in SPS hold time, as noted in Table II. The carbon nanotubes were present in the alumina grain boundaries as well as between the niobium particles and the alumina matrix. Agglomerates of carbon nanotubes ranged from tens of nanometers to a few microns in width and there was evident porosity. The majority of cracks and pores were seen at the alumina-carbon nanotube interfaces and crack bridging was seen in a few circumstances, as seen in Fig.5.

Analyses of the post-mortem fracture surfaces indicate two distinct failure modes of the niobium particles. Both of which are apparent on the niobium particle in Fig. 6. First, some of the niobium regions completely debonded from the brittle alumina matrix. And in some cases, imprints of the

small alumina grains can be seen in the region of debonding (indicated by the black arrow in Fig. 6). Second, it is apparent that the majority of the niobium particles tended to fracture in a brittle manner that is typical for body-centered cubic and high melting temperature metals like niobium. Cleavage fracture and the presence of river lines indicate that the niobium particles ultimately failed without much plasticity. Such behavior is seen in the lower half of the niobium particle in Fig. 6.

The resulting bend fracture toughness of 6.1 $MPa \cdot m^{1/2}$ in the 10 vol%Nb-alumina system indicates that the niobium regions did, indeed, absorb some energy from the propagating crack. Since this energy was not used to plastically deform the niobium, the crack propagation resistance is attributed to crack blunting and crack bridging. Such crack-tip shielding toughening mechanisms have been observed Nb_3Al composites reinforced with Nb particulate [33].

Observations and measurement of stable crack growth allows for the development of an R-curve. However, even with the smallest displacement rates, the three-point bend samples failed catastrophically. A bias-notched (cut diagonally) sample was also fabricated to allow for a decreasing *K*-field situation by creating a situation where the crack grew into an increasing wedge of material. The sample was tested under identical loading conditions and no stable crack growth was observed [34].

However, upon analysis of the images taken before and after fracture, we identified the crack that initiated failure and found that subcritical growth (and any observable R-curve behavior) occurred during the first 3 μm of crack growth. With a notch radius of ~ 30 μm, it is highly improbable that we could identify the exact region of failure and image it with adequate resolution for R-curve development. We conclude that nanocrystalline alumina is too brittle to allow for R-curve measurement with the current or any experimental setup. Thus, for all practical purposes, nanocrystalline alumina reinforced with niobium or carbon nanotubes does not show R-curve behavior.

3.4. Comparative Discussion

Inspection of literature [16-25] exposes some inconsistency amongst the groups studying carbon nanotube-reinforced alumina composites – in particular those measured by SEVNB techniques. For example, Fan *et al.* fabricated 12 vol%MWCNT-alumina composites with fracture toughness of 5.5

$MPa \cdot m^{1/2}$, but Wang et al. reports a mere 3.3 $MPa \cdot m^{1/2}$ when 10 vol%SWCNT was added to alumina. The densities (only 95%) and matrix grain sizes were similar; however, Fan *et al*. used a technique similar to the way the DWCNT-alumina samples were made in this study in order to disperse the carbon nanotubes thoroughly. It is unlikely that the number of walls would contribute to such a difference, but fact that both groups had mere 95% dense specimens could explain the inconsistencies in results. However, it is clear from the carbon nanotube loadings reported that fully dense CNT-alumina composites are not easily obtained over ~10 volume percent CNT loading. This is also consistent with the present study's findings.

In 2003, the present group published fracture toughness data based on the IF method [24]. A 200% increase in fracture toughness with incorporation of 10 vol%SWCNT into nanocrystalline alumina was reported. After publication of the indentation fracture toughness results, a rebuttal paper by Wang *et al*. was published which directly contradicted our findings [23]. Wang et al. claimed to reproduce the Zhan *et al*. study, but with contradictory results. Wang *et al*. employed both the IF and SEVNB techniques to measure the fracture toughness of 10 vol%SWCNT-alumina and they concluded that there was no benefit of adding carbon nanotubes to alumina. However, it is clear from Table III that since their SPS equipment/graphite die was limited to 40 MPa of applied stress, higher temperature and longer hold times were necessary to obtain high density. Consequently, their matrix grain size was thousands of nanometers and they were only able to obtain a 95% dense sample – very unlike the microstructure originally reported on by Zhan *et al*., which was 100% dense.

The porosity and surface finish play very important roles in the mechanical properties of ceramics, particularly hardness and indentation fracture toughness. It is clear from Fig. 7 that very little load transfer from the matrix to the carbon nanotubes could be expected from an 86% dense sample. The standard for using the Vickers indentation method to quantify hardness specifically calls for finer than 1μm surface finish and states that porosity may interfere with measuring indents properly. Fig. 8a is an image of Wang *et al*.'s Vickers indent on 10 vol%SWCNT-alumina published in ref. [23]. The surface finish of their composites was not acceptable for application of the Vickers method, large pores were present in the sample. The indentation load was accommodated by pore collapse and no cracks evolved from the indent corners. In contrast, the nanocomposites fabricated by Zhan *et al.* possessed very little porosity and the cracks emitted from the indent corners could be

easily be measured (Fig. 8b). The indentation load was clearly accommodated by pore collapse and development of a radial crack was not possible.

Table III. Comparison of Mukherjee vs. Wang SWCNT-alumina investigation

Comparison Parameters	***A.K. Mukherjee's group* [24]**	***Wang et al.*** [23]
Starting Materials	SWCNT + Al_2O_3	SWCNT + Al_2O_3
Dispersion & Mixing Methods	Wet-milling & Sieving	No sieving
SPS Processing Conditions	SPS 1150°C/3min 63 MPa	SPS 1450-1550°C/ 3-10 min, 40 MPa
Relative Density	100	95.1
Grain Size [nm]	~200	1000-2000
Fracture Toughness	194% increase (IF)	No toughening (IF & SEVNB)

In addition, the present study determined via Raman spectroscopy that the carbon nanotubes begin to break down at temperatures above ~1250°C. To positively prove that Wang *et al*. could not expect to have retained the carbon nanotubes in their samples, a sample was consolidated in the SPS at 1550°C for 5 minutes. Fig. 2 clearly shows that there is no splitting of the G-band and the intensities of the D and G-bands grown more close in amplitude; both signaling loss of carbon nanotube structure and creation of disordered graphite.

Like the present study, Wang *et al*. also applied the SEVNB technique to measure fracture toughness. Unlike the discrepancies in the IF data, both of our groups obtained similar SEVNB results for 10 vol%SWCNT-alumina; Wang *et al*. reported 3.3 $MPa \cdot m^{1/2}$ and the present study reports 2.76 $MPa \cdot m^{1/2}$. Interestingly, the 5 vol%DWCNT-alumina samples tested with the SEVNB in the present study were exactly what Wang *et al*. measured (3.33 $MPa \cdot m^{1/2}$) for their 10 vol%SWCNT-alumina samples. Consequently, most groups (including the present study) that have reported SEVNB fracture toughness data have found that CNT-alumina systems have similar fracture toughness to intrinsic alumina.

Fibers are added to matrices for strengthening and toughening via fiber bridging – a crack wake or extrinsic toughening phenomenon. Commonly, the amount of toughening increases with the volume content of fibers because the number of fibers bridging the crack wake increases as fiber

loading increases. Carbon nanotubes were selected because they have incredible combination of tensile strength and flexiblility. However, as depicted by the SEVNB testing, the carbon nanotubes provided negligible toughening. This may be attributed to the nanoscale nature of the carbon nanotubes and/or a very weak interaction (*i.e.* negligible traction forces) between the nanotubes and alumina matrix. Strengthening the interface between the carbon nanotubes and alumina by means of surface functionalization may result in some measurable extrinsic toughening. This phenomenon could theoretically be measured by methods that can achieve stable crack growth and obtainment of an R-curve (stress intensity vs. crack extension). R-curves can be obtained using standard bend testing or compact tension (C(T)) techniques, in which the load is incrementally increased during stable crack growth and the crack length recorded. From the recorded loads and crack measurements, the stress intensity K vs. Δa (crack extension) curve can be generated.

Unfortunately, stable crack growth is very difficult to obtain in nanocrystalline ceramics. In our study, disk-shaped samples of pure alumina and 5 vol%SWCNT-alumina were tested with using the C(T) technique (ASTM 399). Stable crack growth, and, hence, development of an R-curve, could not be obtained in either system. It is clear that the nanocrystalline alumina matrix was too brittle to measure the extrinsic toughening expected from grain and fiber bridging.

Comparing results from various investigators throughout literature [1-25] should be done so with great caution in that different methods were used to evaluate the fracture toughness of CMC. As mentioned previously, the indentation method (IF) for calculation of fracture toughness can be misleading and inaccurate in composites. The equations used to estimate the fracture toughness are not based on specific stress conditions, but were merely derived from curve-fitting of data obtained from monolithic ceramics [26]. This highlights the necessity of enforcing that researchers must use ASTM *standard* techniques (*not* IF) to evaluate the mechanical properties of advanced ceramics, and especially their composites. For example, the use of ASTM C1421 for “Standard Test Methods for Determination of Fracture Toughness of Advanced Ceramics at Ambient Temperatures”. This would ensure that only accurate data be presented to the scientific community - allowing for meaningful comparison across material systems, processing routes and most importantly amongst different researchers.

4. Conclusions

Alumina-based nanocomposites were successfully fabricated using advanced powder processing techniques (i.e. HEBM and cryomilling) and consolidated using SPS. In just a few minutes, fully dense (greater than 98.5 %TD) niobium and/or carbon nanotube-reinforced alumina nanocomposites were achieved. Raman spectroscopy verified that carbon nanotubes were preserved after sintering within the SPS at 1150°C. However, it was also found that SWCNTs are destroyed if sintered at 1350°C. Thus, it is advised that consolidation temperatures be limited to ~1250°C when SWCNTs are present within the sample. NMR showed that no Al_4C_3 was formed in SWCNT-alumina nanocomposites – even after consolidation at 1500°C for 10 mins. Thus, the SWCNT-alumina is purely a physical mixture and no chemical bonding occurs between the carbon nanotubes and alumina. The structural perfection of SWCNTs have not been compromised and they remain as ultra-strong fibers.

SPS results in anisotropic mechanical properties in alumina nanocomposites due to residual stresses and preferential alignment of CNT or Nb agglomerates perpendicular to the pressing direction. A 103% difference in fracture toughness between sample orientations (surface vs. cross section) was measured using the Vickers indentation method in the 5 vol%DWCNT-alumina samples. Single-edge V-notched bend testing was used to measure the fracture toughness of alumina-based nanocomposites. The four-point bend fracture toughness of 5 and 10 vol%SWCNT-alumina were within experimental error of pure alumina (~3 $MPa \cdot m^{1/2}$). However, CNTs can be added to nanocrystalline alumina without degrading the fracture toughness, with the added benefit of anisotropic electrical and thermal properties [35,36]. As with the measurements using four-point bending, the samples consolidated from cryomilled and HEBM powders had an average fracture toughness of 3.9 and 3.5 $MPa \cdot m^{1/2}$, respectively. Thus, 10 vol%Nb was successful in toughening nanocrystalline alumina (~6 $MPa \cdot m^{1/2}$ via three-point bend testing) and is the best candidate for load bearing applications.

Fiber bridging (CNTs) and ductile phase toughening (Nb) are extrinsic toughening mechanisms that can only be measured using a method that is capable of obtaining stable crack growth. *In situ* three-point bend tests were performed on pure alumina and various alumina-nanocomposites in

attempt to directly observe toughening mechanisms and to obtain the R-curve (extrinsic portion of fracture toughness) of these CMC. No subcritical crack growth was obtained because the alumina nanocomposites were still too brittle. Thus, it was concluded that niobium/carbon nanotube-reinforced alumina nanocomposites do not possess any R-curve behavior.

Controversy remains about the effectiveness of carbon nanotube additions to alumina. Controversy will remain until the advanced ceramic community demands that researchers report mechanical properties obtained only from ASTM standard testing techniques (*i.e.* ASTM C1421). Specifically, measuring a CMC's fracture toughness using non-standard Vickers indentation technique is not accurate in that it was developed from a set of monolithic curve fittings and unrepeatable stress conditions [26]. Finally, Raman Spectroscopy must be used to verify the preservation of CNTs before reporting to literature.

Acknowledgements

This research was supported by a grant (# W911NF-04-1-0348) from the Army Research Office.

References

1. Tuan, W.H. and R.J. Brook, *The toughening of alumina with nickel inclusions.* Journal of the European Ceramic Society, 1990. **6**(1): p. 31-37.
2. Ji, Y. and J.A. Yeomans, *Processing and mechanical properties of Al2O3-5 vol.% Cr nanocomposites.* Journal of the European Ceramic Society, 2002. **22**(12): p. 1927-1936.
3. Mishra, R.S. and A.K. Mukherjee, *Processing of high hardness-high toughness alumina matrix nanocomposites.* Materials Science and Engineering A, 2001. **301**(1): p. 97-101.
4. Garcia, D.E., S. Schicker, J. Bruhn, R. Janssen and N. Claussen, *Processing and Mechanical Properties of Pressureless-Sintered Niobium-Alumina-Matrix Composites.* Journal of the American Ceramic Society, 1998. **81**: p. 429-461.
5. Diaz, L.A., A.F. Valdes, C. Diaz, A.M. Espino and R. Torrecillas, *Alumina/molybdenum nanocomposites obtained in organic media.* Journal of the European Ceramic Society, 2003. **23**(15): p. 2829-2834.
6. Nawa, M., T. Sekino and K. Niihara, *Fabrication and mechanical behavior of Al2O3/Mo nanocomposites.* J. Mater. Sci., 1994. **29**: p. 3185-3192.
7. Sekino, T., T. Nakajima, S. Ueda and K. Niihara, *Reduction and sintering of a nickel-dispersed-alumina composite and its properties.* J. Am. Ceram. Soc.,1997. **80**: p. 1139-1148.
8. Kim, Y.D., S.-T. Oh, K.H. Min, H. Jeon and I.-H. Moon, *Synthesis of Cu dispersed Al2O3 nanocomposites by high energy ball milling and pulse electric current sintering.* Scripta Materialia, 2001. **44**(2): p. 293-297.
9. Oh, S.-T., T. Sekino and K. Niihara, *Fabrication and mechanical properties of 5 vol% copper dispersed alumina nanocomposite.* Journal of the European Ceramic Society, 1998. **18**(1): p. 31-37.
10. Rousset, A., *Alumina-Metal (Fe, Cr, Fe0.8Cr0.2) Nanocomposites.* Journal of Solid State Chemistry, 1994. **111**(1): p. 164-171.
11. Qin, X.Y., R. Cao and H.Q. Li, *Fabrication and mechanical properties of ultra-fine grained [gamma]-Ni-20Fe/Al2O3 composites.* Ceramics International, 2006. **32**(5): p. 575-581.
12. Anya, C.C., *Microstructural nature of strengthening and toughening in Al2O3-SiC(p) nanocomposites.* Journal of Materials Science, 1999. **34**(22): p. 5557-5567.
13. Zhu, W.Z., H.G. J and S.D. Z, *Microstructure and mechanical properties of a Si3N4/Al2O3 nanocomposite.* Journal of Materials Science, 1997. **32**(2): p. 537-542.
14. Acchar, W., C.A. Cairo and A.M. Segadaes, *Effect of tungsten carbide additions on the microstructure and properties of hot-pressed alumina.* Materials Science and Engineering: A, 2005. **406**(1-2): p. 74-77.
15. Sarkar, D., S. Adak and N.K. Mitra, *Preparation and characterization of an Al2O3-ZrO2 nanocomposite, Part I: Powder synthesis and transformation behavior during fracture.* Composites Part A: Applied Science and Manufacturing, 2007. **38**(1): p. 124-131.
16. Cha, S.I., K.T. Kim, K.H. Lee, C.B. Mo and S.H. Hong, *Strengthening and toughening of carbon nanotube reinforced alumina nanocomposite fabricated by molecular level mixing process.* Scripta Materialia, 2005. **53**(7): p. 793-797.
17. Flahaut, E., A. Peigney, C. Laurent, C. Marliere, F. Chastel and A. Rousset, *Carbon nanotube-metal-oxide nanocomposites: microstructure, electrical conductivity and mechanical properties.* Acta Materialia, 2000. **48**(14): p. 3803-3812.
18. Sun, J., L. Gao and X. Jin, *Reinforcement of alumina matrix with multi-walled carbon nanotubes.* Ceramics International, 2005. **31**(6): p. 893-896.

19. Mo, C.B., S.I. Cha, K.T. Kim, K.H. Lee and S.H. Hong, *Fabrication of carbon nanotube reinforced alumina matrix nanocomposite by sol-gel process.* Materials Science and Engineering A, 2005. **395**(1-2): p. 124-128.

20. An, J.W., D.H. You and D.S. Lim, *Tribological properties of hot-pressed alumina-CNT composites.* Wear, 2003. **255**(1-6): p. 677-681.

21. Fan, J., D. Zhao, M. Wu, Z. Xu and J. Song, *Preparation and Microstructure of Multi-Wall Carbon Nanotubes-Toughened Al2O3 Composite*. J. Amer. Ceram. Soc, 2006. **89**(2): p. 750-753.

22. Siegel, R.W., S.K. Chang, B.J. Ash, J. Stone, P.M. Ajayan, R.W. Doremus and L.S. Schadler, *Mechanical behavior of polymer and ceramic matrix nanocomposites.* Scripta Materialia, 2001. **44**(8-9): p. 2061-2064.

23. Wang, X., N.P. Padture and H. Tanaka, *Contact-damage-resistant ceramic/single-wall carbon nanotubes and ceramic/graphite composites.* Nat Mater, 2004. **3**(8): p. 539-544.

24. Zhan, G.-D., J.D. Kuntz, J. Wan and A.K. Mukherjee, *Single-wall carbon nanotubes as attractive toughening agents in alumina-based nanocomposites.* Nat Mater, 2003. **2**(1): p. 38-42.

25. Jiang, D., K. Thomson, J.D. Kuntz, J.W. Ager and A.K. Mukherjee, *Effect of sintering temperature on a single-wall carbon nanotube-toughened alumina-based nanocomposite.* Scripta Materialia, 2007. **56**(11): p. 959-962.

26. Quinn, G.D. and R.C. Bradt, *On the Vickers Indentation Fracture Toughness Test.* J. Am. Cer. Soc., 2007. **90**(3): p. 673-680.

27. Chen, W., U. Anselmi-Tamburini, J.E. Garay, J.R. Groza and Z.A. Munir, *Fundamental investigations on the spark plasma sintering/synthesis process: I. Effect of dc pulsing on reactivity.* Materials Science and Engineering A, 2005. **394**(1-2): p. 132-138.

28. Shen, Z., M. Johnsson, Z. Zhao and M. Nygren, *Spark Plasma Sintering of Alumina.* Journal of the American Ceramic Society, 2002. **85**: p. 1921-1927.

29. Antsis, G.R., Chantikul, P., Marshall, D.B., and B.R. Lawn, *A critical evaluation of indentation techniques for measuring fracture toughness: I. Direct Crack Measurement.* Amer. Ceram. Soc., 1981. **64**: p.533-538.

30. Saito, R., Dresselhaus, G., and Dresselhaus, M.S., *Physical Properties of Carbon Nanotubes*. 1998, London: Imperial College Press. 183-206.

31. Jiang, D., K. Thomson, J.D. Kuntz, J.W. Ager and A.K. Mukherjee, *Effect of sintering temperature on a single-wall carbon nanotube-toughened alumina-based nanocomposite.* Scripta Materialia, 2007. **56**(11): p. 959-962.

32. Flahaut, E., A. Peigney, C. Laurent, C. Marliere, F. Chastel and A. Rousset, *Carbon nanotube-metal-oxide nanocomposites: microstructure, electrical conductivity and mechanical properties.* Acta Materialia, 2000. **48**(14): p. 3803-3812.

33. Bencher, C.D., Sakaida, A., Venkateswara Rao, K.T., Ritchie, R.O., *Toughening Mechanisms in Ductile Niobium-Reinforced Niobium Aluminide (Nb/Nb3Al) In Situ Composites.* Metall. Mater. Trans. A., 1995. 26A: p. 2027-2033.

34. Thomson, K.E., D. Jiang, J.A. Lemberg, K.J. Koester, R.O. Ritchie and A.K. Mukherjee, *In-situ bend testing of niobium-reinforced alumina nanocomposites with and without single-walled carbon nanotubes.* Mat. Sci. & Eng. A, 2008, 493, p. 256-260.

35. Zhan, G.-D. and A.K. Mukherjee, *Processing and characterization of nanoceramic composites with interesting functional and structural properties.* Rev. Adv. Mat. Sci., 2005. **10**: p. 185-196.

36. Zhan, G.-D., J.D. Kuntz, A.K. Mukherjee, P. Zhu and K. Koumoto, *Thermoelectric properties of carbon nanotube/ceramic nanocomposites.* Scripta Materialia, 2006. **54**(1): p. 77-82.

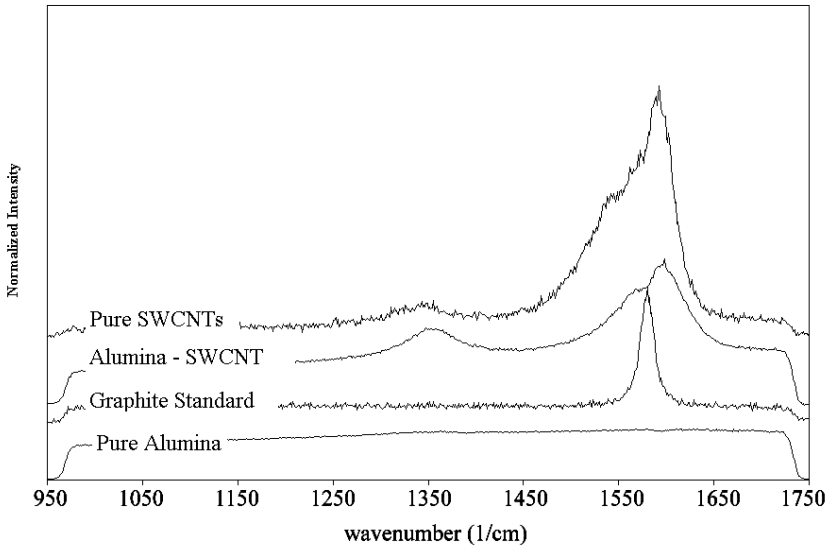

Fig. 1. Pulsed Laser Raman Spectroscopy comparing graphite, SWCNT and alumina starting powders with our 10 vol%SWCNT-alumina nanocomposite (SPS: 1150°C, 3 min)

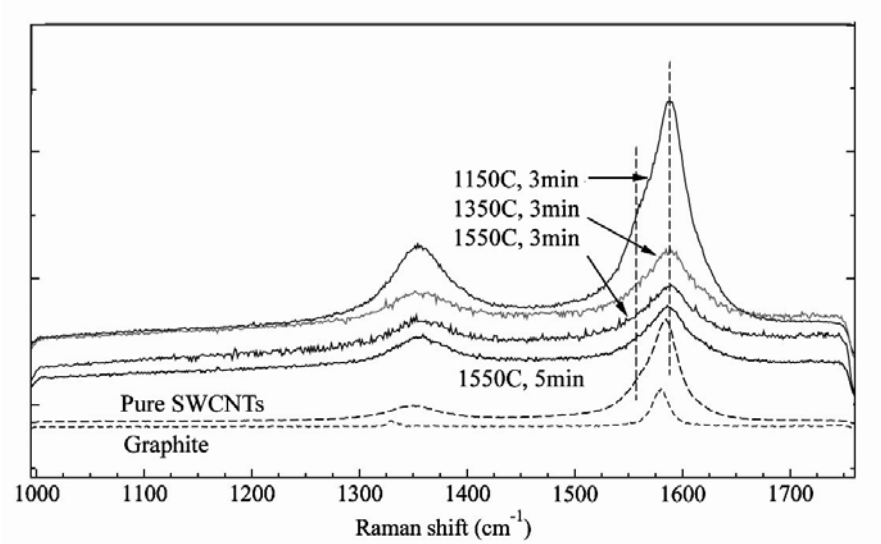

Fig. 2. Pulsed Laser Raman study of SWCNT-Alumina nanocomposites for determination of carbon nanotube degradation temperature as a function of SPS temperature and time [25]

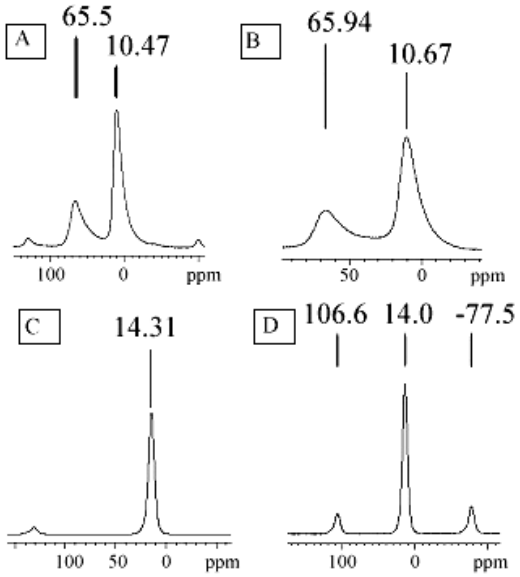

Fig. 3. ^{27}Al MAS NMR spectra showing: a) As-received alumina, b) HEBMed alumina, c) pure alumina SPSed at 1200°C for 4 minutes, and d) 5 vol%SWCNT-alumina SPSed at 1200°C for 6 minutes. (10-14 ppm = 6 coordinated and ~66 ppm = 4 coordinated)

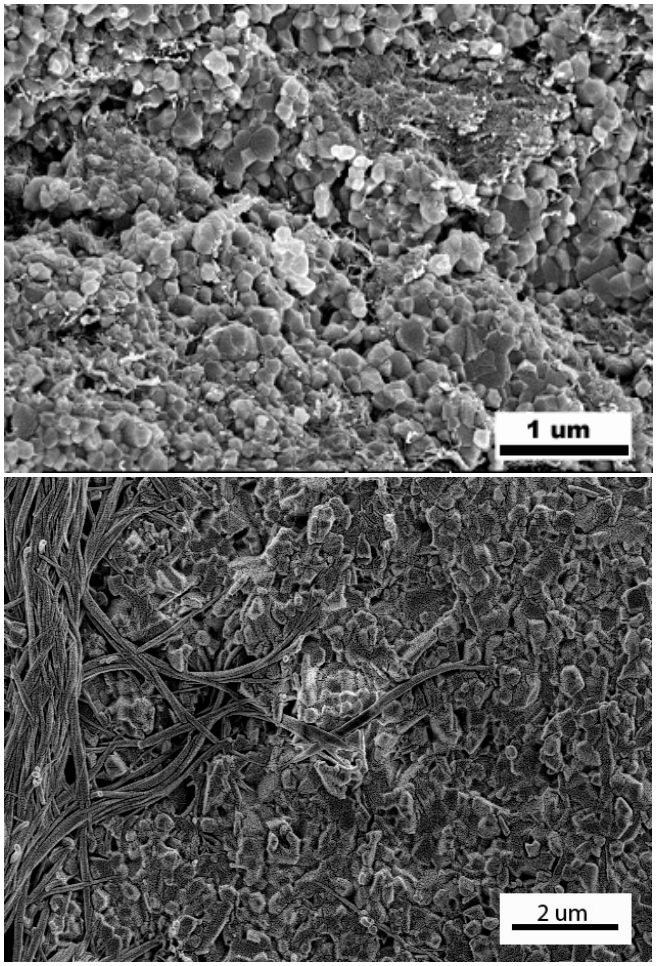

Fig. 4. SEM images of fracture surfaces of 5 vol%SWCNT-alumina (top) and 5 vol%DWCNT-alumina (bottom)

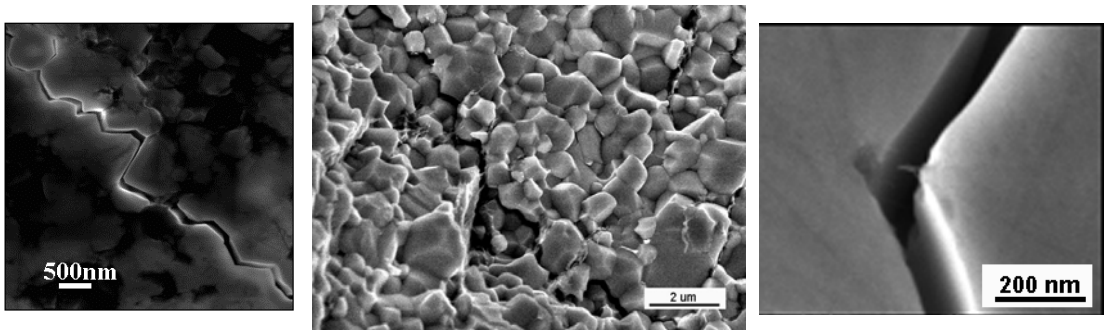

Fig.5. SEM images illustrating the 3 ways in which fibers may toughen the alumina matrix by energy dissipation.

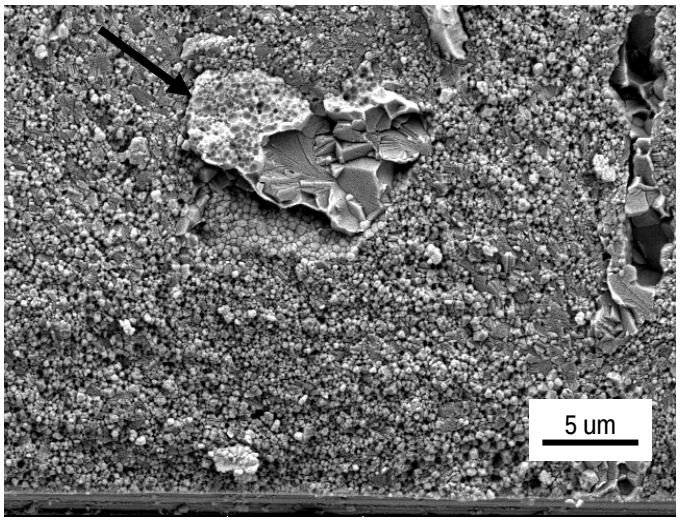

Fig. 6. SEM image of 10 vol%Nb-Al2O3 fracture surface (Au coated) displaying two modes of failure – particle debonding (arrow) and cleavage fracture.

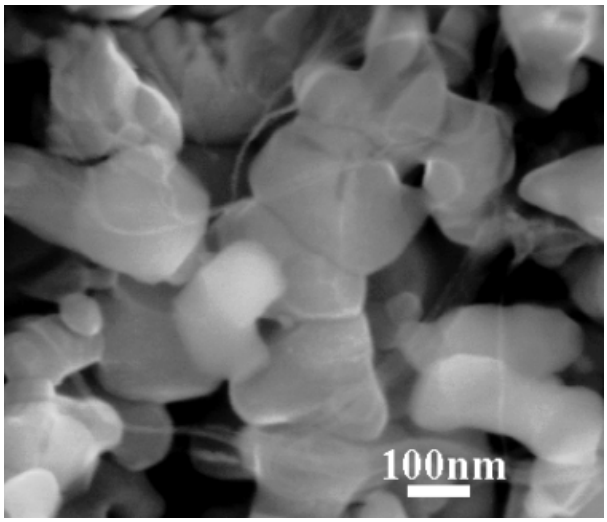

Fig. 7. High-resolution SEM image of an 86% dense 10 vol%SWCNT-alumina sample showing little potential for load transfer and toughening from the nanotubes

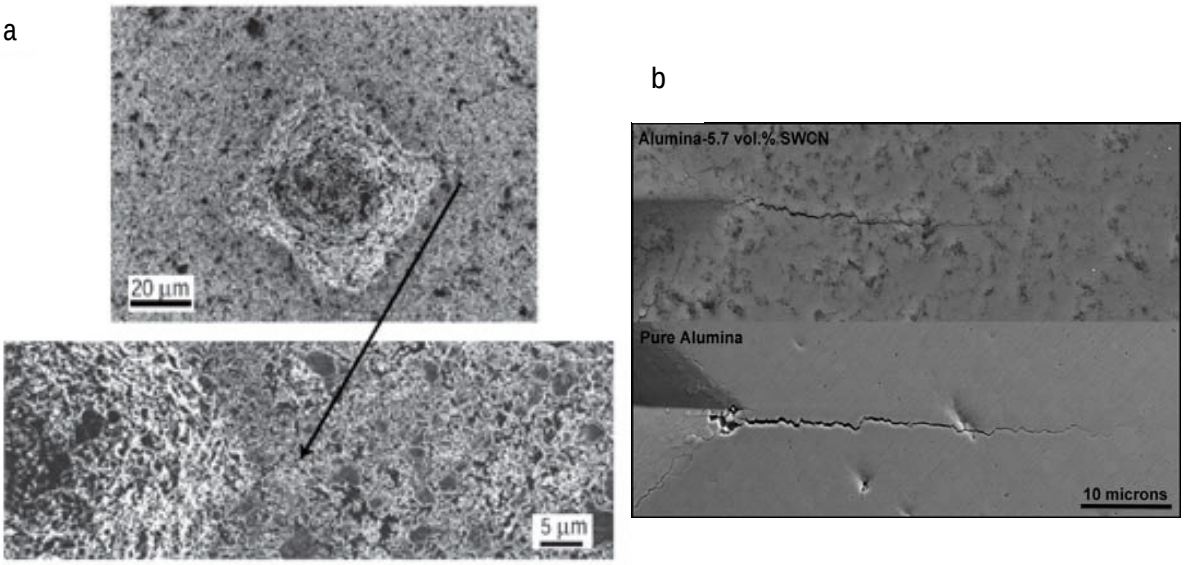

Fig. 8. Vickers indents from a) Wang et al.'s *Nature Materials* paper showing no crack generation on 10 vol%SWCNT-alumina (95% dense) [23] and Zhan et al's [24]